Contents lists available at ScienceDirect

Journal of Contaminant Hydrology

journal homepage: www.elsevier.com

Adsorption and removal of phenoxy acetic herbicides from water by using commercial activated carbons: experimental and computational studies

Agustín Spaltro[a, b], Matías Pila[a, b], Sandra Simonetti[c, d, *], Silvia Álvarez-Torrellas[e], Juan García Rodríguez[e], Danila Ruiz[a, b], Andres Díaz Compañy[c, f], Alfredo Juan[c], Patricia Allegretti[a]

[a] CEDECOR (Centro de Estudio de Compuestos Orgánicos), Facultad de Ciencias Exactas, Universidad Nacional de La Plata (UNLP), Calle 115 y 47, 1900 La Plata, Argentina
[b] CONICET (Consejo Nacional de Investigaciones Científicas y Técnicas), Argentina
[c] Instituto de Física del Sur (IFISUR), Departamento de Física, Universidad Nacional del Sur (UNS), CONICET, Av. L.N. Alem 1253, B8000CPB Bahía Blanca, Argentina
[d] Universidad Tecnológica Nacional (UTN), 11 de Abril 461, B8000LMI Bahía Blanca, Argentina
[e] Grupo de Catálisis y Procesos de Separación (CyPS), Departamento de Ingeniería Química y de Materiales, Facultad de Ciencias Químicas, Universidad Complutense de Madrid, Avda. Complutense s/n, 28040 Madrid, Spain
[f] Comisión de Investigaciones Científicas (CIC), Calle 526 e/10 y 11, 1900 La Plata, Argentina.

ARTICLE INFO

Keywords:
Activated carbon
Adsorption
Computational simulation
Phenoxy acetic herbicides

ABSTRACT

In this study, commercial activated carbons (GAB and CBP) were successfully used for the removal of two phenoxy acetic class-herbicides, 4-chloro-2-methyl phenoxy acetic acid and 2.4-dichlorophenoxy acetic acid (MCPA and 2.4-D) from aqueous solution. The adsorbent materials were characterized, and their equilibrium adsorption capacity was evaluated. The results suggest that the microporous properties of GAB activated carbon enhanced the adsorption capacity, in comparison to CBP carbon. Thus, the increasing in the ionic strength favored the adsorption removal of both pesticides, indicating that electrostatic interactions between the pollutant and the adsorbate surface are governing the adsorption mechanism, but increasing pH values decreased adsorption capacity. Experimental data for equilibrium was analyzed by two models: Langmuir and Freundlich. Finally, computational simulation studies were used to explore both the geometry and energy of the pesticides adsorption.

1. Introduction

The removal of hazardous organic compounds from contaminated water by feasible and clean technologies is one of the most important issues in water treatment research. Pesticides are one of the most widely used contaminants in many countries, especially where the main economic sources are agro-industrial activities, such as Argentina, Brazil, Chile, India, etc. Thus, the contamination of natural water and groundwater by pesticide compounds is a worldwide problem that has become an important challenge for scientists and legal authorities. Clean water is one of the most important issues due to the continuing world economic development, the steady increase in the global population and the shortage of this non-renewable resource due to climate change. For decades, tons of biologically active substances, synthesized for their use in agriculture, industry, medicine, etc., have been dumped into the environment inadequately.

Phenoxy herbicides, one of the most widely used family of herbicides, have been commercially available for many years. 2.4-D was first used in the US in the 1940s. This agrochemical is a systemic herbicide which selectively kills most broadleaf weeds by causing uncontrolled growth in them, but leaves most grasses such as cereals, lawn turf, and grass land relatively unaffected. These compounds are used in corn, maize and grazing land cultivation and have furthermore been used as defoliating agents as well as for the removal of water weeds. This agrochemical is an herbicide that kills plants by changing the way certain cells grow. 2,4-D comes in several chemical forms, including salts, esters, and an acid form.

* Corresponding author at: CEDECOR (Centro de Estudio de Compuestos Orgánicos), Facultad de Ciencias Exactas, Universidad Nacional de La Plata (UNLP), Calle 115 y 47, 1900 La Plata, Argentina.
Email address: ssimonet@uns.edu.ar (S. Simonetti)

https://doi.org/10.1016/j.jconhyd.2018.10.003
Received 28 August 2018; Received in revised form 6 October 2018; Accepted 10 October 2018
Available online xxx
0169-7722/

The toxicity of 2.4-D depends on its form. The form also affects what will happen to 2.4-D in the environment and what impacts it may have, especially on fish. 2.4-D is used in many products to control weeds, and it is often mixed with other herbicides in these products. In 1987, the International Agency for Research on Cancer (IARC) stated that 2.4-D is a β-2 carcinogenic compound (IARC monographs on the evaluation of carcinogenic risks to humans: an updating of IARCMonographs, Supplement 7, n.d.). Recently, this herbicide has been classified as a group D carcinogen by USEPA and is suspected to be an endocrine disruption compound (EPA, 2007). It has been demonstrated that acts increasing abnormal sperms and sperms immobility, the probability of immune deficiency disorders and the incidence of nervous, kidney and respiratory diseases. In addition, fetus mortality, urinary system disorders, and congenital diseases have also been observed in the exposed animals to this pollutant (Forest Health Protection, 2006).

4-chloro-2-methyl phenoxy acetic acid (MCPA) is a selective herbicide with systemic and hormonal action for the control of broadleaf weeds in cereals and other crops. It belongs to the group of hormonal herbicides, so-called because they affect the physiology of the plants in the same way as natural auxins (in dole acetic acid), but in an exaggerated way and without control. It was registered in Canada for use in agricultural sites, fine grass and in forestry and currently it is found among the 10 most important pesticides used in Europe (Fielding et al., 1992). In the United States, it is classified as a restricted use pesticide. Within this country, the Environmental Protection Agency (EPA) classifies MCPA as a potential pollutant of groundwater, with an estimated environmental concentration of 47.3 $mg \cdot l^{-1}$ for underground drinking water sources for use without risk to human health; also, it is considered as a possible carcinogenic and mutagenic compound by the International Agency for Research on Cancer. As a post-emergence herbicide (Tomlin, 1994), it is used when the crop is already born, usually during its first stages. Although it is not extremely toxic, it has recently been determined that MCPA can form complexes with metal ions and therefore increase their bioavailability (Kobylecka et al., 2003; Kruszynski et al., 2002). Therefore, its DT_{50} value on the ground, at 20 °C, is 24 days, while in water is only of 13.5 days. The carboxyl group present in its chemical composition is mainly responsible for its relatively high chemical activity and dominates all interactions with mineral surfaces. The MCPA is very poorly soluble in water and due to its anionic nature, is weakly retained by most of the soil components, remaining dissolved with a high probability of draining and leaching to ground and surface water.

Many techniques have been developed for pesticides removal from water. Adsorption has been revealed as a promising method for phenoxy acetic herbicides depletion due to its simple, economic and environmental friendly characteristics. Carbon materials constitute the most widely used as adsorbents in the removal of organic compounds from water. Commercially, the available activated carbons (AC) come from natural products such as wood and fruit peel. But also, any material that is abundant in carbon is likely to be a precursor of this material. In this work it has been used two commercial activated carbons, GAB and CBP, as efficient and economical materials for the removal of both pesticides.

2. Materials and methods

2.1. Adsorbates

Both pesticides were synthesized from bibliographic data (Budaver, 1989; Organic Syntheses, 1973; Buckles and Wawzonek, 1948) and purified by recrystallization from water until verifying that their physical constants are constant and by checking into an HP5890 Gas Chromatograph coupled to an HP 5972 and a mass selective detector with an HP5-MS column, 30 m × 0.25 mm × 5 μm, using helium as a carrier gas and a flow rate of 0.6 $ml \cdot min^{-1}$. Molecular structures and acid-base equilibrium of both substances are shown in Fig. 1 and the dissociation diagrams are shown in Fig. 1, where it can be observed that the pKa values of 2.4-D and MCPA were of 2.73 and 3.07, respectively. Finally, the most important physicochemical properties of both pesticides are summarized in Table 1.

Since both molecular structures are very similar, their molecular size is very similar. The most important difference between the compounds lies in their solubility in water, higher for MCPA pollutant.

2.2. Adsorbents

Two commercial activated carbons, with different physical and chemical properties, named as GAB and CBP, were tested. The adsorbents were ground and sieved to the required particle size (500–355 μm). Firstly to be used in the adsorption tests, the materials were thoroughly washed with boiling water, in order to remove impurities from the inner pores and then were dried in an oven at 110 °C for 24 h.

2.3. Adsorbents characterization

The adsorbent materials used in the adsorption experiments were characterized to detail their surface and morphological chemical properties. The textural characterization of the solids was carried out by N_2 adsorption–desorption isotherms in an auto-

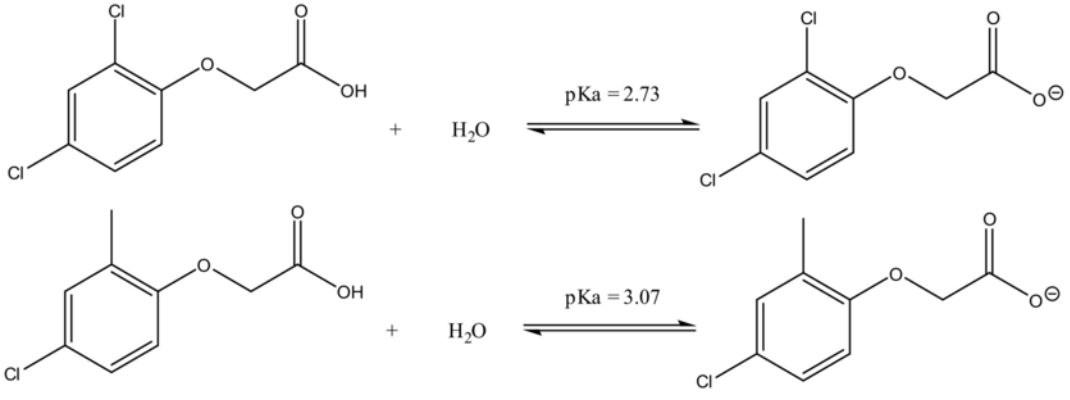

Fig. 1. Acid-base equilibrium of 2.4 – D and MCPA.

Table 1
Physicochemical properties of the tested herbicides.

Herbicide	Molecular weight ($molg^{-1}$)	Solubility in H_2O (mgL^{-1})at 298 K	Molecular size (nm^3)
2.4-D	221	500	0.1000
MCPA	200	825	0.0964

mated physisorption equipment (Micromeritics ASAP 2020) at 77 K. The specific surface area and pore size values were determined by using BET equation from N_2 adsorption isotherm data. The total pore volume was calculated from the amount of N_2 adsorbed at $P/P_0 = 0.95$, while the micropore volume was estimated by the Dubinin-Radushkevich method. The mesopore volume is also obtained from the N_2 adsorption isotherm in the range of relative pressures P/P_0 from 0.40 to 0.95 assuming that the molar volume of liquid nitrogen is 35 $cm^3 \cdot mol^{-1}$. Likewise, the medium pore size of the materials was obtained by using the Density Functional Theory (DFT) and Barrett, Joyner and Halenda (BJH) method (Barrett et al., 1951; Galarneau et al., 2014).

Attending to explore the surface chemistry of the materials, FT-IR spectra of the solids were recorded in a Thermo Nicolet spectrophotometer within the range of 400–4000 cm^{-1}using the KBr pellet technique. The zero-charge point (pH_{PZC}) was determined using the mass titration method, in accordance to ASTM D3838–05 (Standard Test Method for pH of Activated Carbon). This methodology is based on the measurement of the pH solution as a function of the mass concentration of the solid (Babic et al., 1999). For this purpose, samples of dried activated carbon ranging from 0.1 to 1.0 g were placed in a flask. Then, 40 mL of previously boiled distilled water were added. The system was boiled for 15 min approximately. Then, the system was disassembled and immediately collected the filtrate and measured the pH at 50 ± 5 °C. Finally, pH values were plotted as a function of the mass percentage, and the point of zero charge was determined by extrapolation to zero mass percentage. Also, Boehm titration measurements were performed in order to determine the acidic and basic surface groups of the activated carbons (Boehm, 1994). Two bases were used for this purpose: NaOH and $NaHCO_3$. It is assumed that $NaHCO_3$ neutralizes only carboxyl groups while NaOH neutralizes carboxylic acids, phenols, lactones and carbonyls. HCl solution was used for the neutralization of the basic groups. In the procedure, 0.1000 g of carbon was placed in a 100 mL Erlenmeyer flask. Then, 100 mL of 0.0563 M HCl solution was added. The system was kept under constant stirring for 24 h. After, the mixture was filtered and 20 mL of each solution was taken. They were titrated with 0.0539 M NaOH using phenolphthalein as pH indicator. For the determination of the acidic groups, two measurements were made following the same procedure, using 0.0539 M NaOH and 0.0500 M $NaHCO_3$, and methyl orange as pH indicator. A blank experiment was also performed in order to verify the pH value of charcoal dispersion in distilled water. Finally, the thermogravimetric analysis (TGA) were carried out under inert conditions (N_2 flow of 50 $mL \cdot min^{-1}$) and with a heating rate of 10 °C min^{-1} from 30 to 1000 °C. The analysis was performed with a Seiko EXTAR 6000 TGA/DTA thermal analyzer.

The morphological properties of the adsorbent materials were explored by scanning electron microscopy (SEM). The micrographs were obtained in JEOL JSM 6400 microscope, equipped with a thermionic cathode electron gun with tungsten filament and a 25 kV detector. Samples, previously dried in an oven overnight at 110 °C, were supported on brass discs by graphite tape.

2.4. Adsorption tests

Batch adsorption studies were carried out by adding a constant dose of activated carbon (0.0020 g) into 25 mL Erlenmeyer flasks containing 20 mL of different initial concentrations (5–40 $mg \cdot L^{-1}$) of MCPA and 2.4-D solutions with a NaCl concentration of 0.01 M for each experiment. Deionized water was used in all the experiments and no buffer solutions were used to avoid the possible formation of precipitates or competition with the solute in the adsorption process. The samples were maintained under constant stirring for 72 h, finding that the adsorption equilibrium was achieved within this time under all the tested operation conditions. MCPA and 2.4-D concentrations were measured in a double beam UV–vis spectrophotometer at 279 and 284 nm, respectively. The equilibrium adsorption capacity, q_e (mgg^{-1}), was calculated according the Eq. 1:

$$q_e = \frac{(C_0 - C_e) \cdot V}{W} \quad (1)$$

where, C_0 and C_e ($mg \cdot L^{-1}$) are the liquid-phase concentrations of pesticide at initial and at equilibrium time, respectively, V (L) is the solution volume and W (g) is the weight of the adsorbent. Each adsorption test was performed in duplicate.

Solution pH is one of the factors that control the adsorption process of organic weak electrolytes on carbon materials due to the formation of electrostatic interactions between the adsorbent and adsorbate. Thus, solution pH determines the carbon surface charge and the dissociation or protonation of the electrolyte. At a solution pH lower than the pH_{PZC} the total or external surface charge, respectively, will be on average positive, whereas at a higher solution pH they will be negative. In addition, the solution pH also controls the dissociation or ionization of the electrolyte through its pKa. Thus, for instance, acidic electrolytes will be dissociated at pH > pKa. Therefore, the solution pH controls the adsorptive–adsorbent and adsorptive–adsorptive electrostatic interactions, which can have a profound effect on the adsorption process.

It is known that the solubility of organic compounds in water is dependent on the concentration of electrolyte present in the aqueous solution. Therefore, ionic strength is a key factor that controls electrostatic interactions. These interactions, whether attractive or repulsive, can be increased or decreased by modifying the concentration of salts dissolved in the medium. When the electrostatic interactions between the surface and the adsorbate are repulsive, an increase in the ionic strength will increase the adsorption capacity. On the other hand, when the interaction is attractive, or the surface concentration is enough low, an increase in the ionic strength will decrease the adsorption removal. There is no single explanation for determining the effect of salt concentration in a given adsorbate-adsorbent system. But it is worth to mention two of them; the so-called salting out and the screening effect. Due to the effect of the salting out an increase in the amount of salt added to the solution generates a decrease in the solubility of the organic molecules in the aqueous phase, increasing the adsorption. The addition of salts to the solution causes its ions to strongly attract water molecules forming hydration spheres, and therefore these water molecules will no longer be available for the dissolution of the organic compound (adsorbate) thus decreasing the solubility of the compound and favoring the diffusion of organic molecules towards the adsorbent. The screening effect can occur with the increase of the salt concentration, thereby decreasing the interactions between the adsorbent and the adsorbate (Bautista-Toledo et al., 2005).

2.5. Computational methodology and model

Density functional theory calculations are performed using the VASP (Vienna Ab initio simulation package) code which is based on the Kohn-Sham density functional theory (DFT) formulation (http://www.vasp.at/, n.d.; Kresse and Hafner, 1993a) and including the dispersion interaction via Grimme's –D2 correction (Grimme, 2006). The electron-ion interactions are described by ultra soft pseudopotentials and exchange correlation energies are calculated with the generalized gradient approximation (GGA) as parameterized by Perdew–Burke–Ernzerhof (Kresse and Hafner, 1993b; Kresse and Hafner, 1994; Perdew et al., 1992; Perdew et al., 1993; Bloch, 1994; Kresse and Joubert, 1999).

The surface chemistry of the activated carbon is dictated by the heteroatoms (carbon (88%), hydrogen (0.5%), nitrogen (0.5%), sulfur (1%), oxygen (7%) and inorganics (3%)) present on it (Pego et al., 2017). Those heteroatoms represent organic functional groups at the edges of carbon surface. The heteroelement content of the carbon depends on its origin and the employed activation method. Because of surfaces diversity, in a first approximation we have selected a graphite model as activated carbon model. Some theoretical studies of graphite (Chen Nand Yang, 1998; Chen and Yang, 1998; Lamoen and BNJ, 1998; Zhu and Lu, 2004; Janiak et al., 1993; Pliego et al., 2005) have confirmed that most of its physics is the same as that of a single graphite layer. In theoretical studies, the structural models that are traditionally used to simulate adsorption are derived from graphite, in which all the atoms are in hexagonal rings (Thomson and Gubbins, 2000). The carbon pores are then assumed to have a slitlike shape confined by the parallel planes of the graphite. According, it was modeled a slab consisting of three graphene layers arranged in a regular hexagonal pattern. The bottom layer of the slab was held fixed allowing the top two layers to relax. The molecule was adsorbed on the topmost surface layer. The vacuum between the slabs when adsorbates are included is greater than 11 Å, large enough to ensure no significant interaction between the slabs. The Brillouin zone of the surface unit cells was sampled with 3x3x1 Monkhorst-Pack mesh. An energy cutoff of 400 eV was used for the bare surface as well as molecules adsorbate on surface. The tolerance for the geometry optimization was set to a force of 0.01 eV/Å and a total energy difference down to ~1 meV/atom. The adsorption energy in each case is calculated according to the following equation $E_{ads} = E_{molecule/\ slab} - E_{molecule} - E_{slab}$, where $E_{molecule}$ is the total energy of an isolated molecule (2,4 -D or MCPA), E_{slab} is the total energy of the bare activated carbon surface and $E_{molecule/\ slab}$ is the total energy of the adsorbate on slab system. A negative Eads corresponds to a stable adsorbate/slab system. Bader analysis was used to calculate the electronic charges on atoms (Bader, 1990).

3. Results and discussion

3.1. Adsorbents characterization

The textural properties, e.g., specific surface area and pore volume of the tested adsorbents are collected in Table 2.

Attending to the specific surface area and pore volume values, commercial activated carbons showed much higher values, e.g., 1189 and 1288 $m^2 g^{-1}$ of BET surface area; 0.53 and 1.10 $cm^3 g^{-1}$ of pore volume for GAB and CBP, respectively.

In Table 3 are summarized the measured concentration of acid and basic groups of GAB and CBP activated carbons. From the results, CBP material contained higher quantity of basic groups than GAB (7.832 *vz.* 2.441 $mmol g^{-1}$), so this adsorbent offered more basic properties on its surface.

Nevertheless, the point of zero charge of GAB adsorbent was found of 7.46, a mainly basic solid, since CBP adsorbent took a value of 4.76, being more acidic. This difference is fundamental to analyze the interactions generated between the adsorbents and both solutes. If the solution pH is higher than 4.76, both the pesticide molecule and CBP surface will be negatively charged, involving repulsive electrostatic forces in the adsorption process, whereas if the solution pH is even higher than 7.46, GAB surface will have a mostly negative charge.

The FT-IR spectra of both activated carbons are shown in Fig. 2. It is noteworthy that both spectra are similar due to the carbonaceous nature of the adsorbents. A high intensity band was observed at 3100–3500 cm^{-1}, corresponding to –OH stretching vibration, due to adsorbed water molecules in the structure of the solid. The bands found at 2850–2920 cm^{-1} are characteristic of the presence of aliphatic groups. These peaks do not show a high intensity, but they are representative of carbon materials. Vibrations at 1600–1610 cm^{-1} and 1461 cm^{-1}detected in the CBP spectrum are indicative of the presence of carboxyl groups (COOH) in the carbon surface. In the range 1000–1260 cm^{-1}, the CBP spectrum showed higher intensity compared to that found for GAB activated carbon, confirming the presence of a higher number of acidic-type functional groups. In the spectrum of CBP activated carbon, a very weak band at 1453 cm^{-1} was observed, attributed to the asymmetric bending of CH_3 groups.

The morphological characterization of activated carbons has been studied by SEM technique. Fig. S2 in the Supplementary Material show the SEM micrographs of both GAB and CBP activated carbons.

TGA curves of both activated carbons can be observed in Fig. S3 (see Supplementary Material). In the temperature range between 80 and 100 °C, the weight loss is attributed to the dehydration of the materials, characteristic of all the solids studied by this technique. The loss of water is very significant for both cases. Throughout the whole temperature range, reaching approximately to 900 °C, the mass loss was very low, indicating that both carbons are very thermally stable.

3.2. MCPA and 2.4-D adsorption tests

In order to study the effect of increasing the electrolyte concentration on the solution, the same adsorption experiments were carried out. Firstly, as expected, it could be confirmed that the modification of the concentration of electrolyte did not affect the equilibrium time.

We separate the results according to the adsorbent and herbicide analyzed.

Table 2
Textural properties of the tested adsorbents.

Adsorbent	S_{BET} ($m^2 g^{-1}$)	$S_{Non\text{-}mic}$ ($m^2 g^{-1}$)	S_{Mic}($m^2 g^{-1}$)	V_{Total} ($cm^3 g^{-1}$)	V_{Mic} ($cm^3 g^{-1}$)	Average pore size* (nm)
CAT	1189	473	580	0.53	0.27	2.25
CBP	1288	1195	99	1.10	0.04	4.39

* Average pore size determined at 4 V/A by BET.

Table 3
Boehm titration results of the GAB and CBP.

Adsorbent	Carboxylic groups ($mmolg^{-1}$)	Phenolic groups ($mmolg^{-1}$)	Basic groups ($mmolg^{-1}$)
GAB	2.721	7.781	2.441
CBP	1.311	7.922	7.832

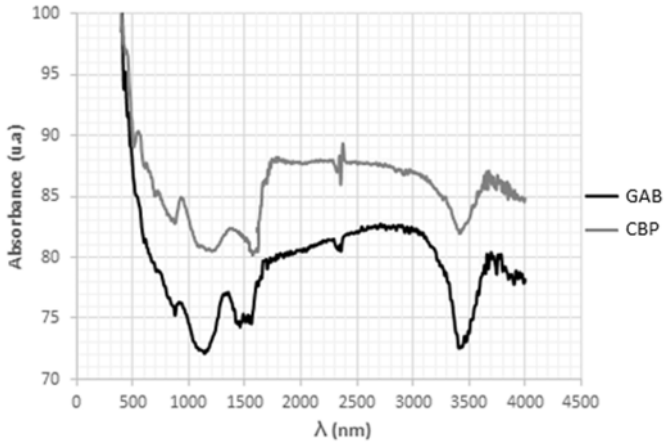

Fig. 2. FT-IR spectra of GAB and CBP activated carbons.

Figs. 3 and 4 show the adsorption isotherms of 2.4–D onto GAB at different pH solution values (5.0; 6.5 and 8.0) and two different ionic strengths (0.01 and 0.50 M, respectively). It can be seen that the increasing in the pH value led to a decreasing in the adsorption capacity. Indeed, at higher ionic strength, the 2.4-D adsorption capacity increased. Figs. 5 and 6 show the results using CBP as adsorbent material; it can be observed the same trend. (See Figs. 7 and 8.)

Comparing the isotherms obtained for the adsorption of 2.4 - D at different values of ionic forces, it can be observed how an increase in this variable generates an increase in the capacity of adsorption on both activated carbons. It is observed that the increase in a first instance is due to the presence of ions in the solution reduces the number of water molecules that can interact with the analyte and this loses the interaction with the medium and is adsorbed by the carbon, this phenomenon disappears when the ionic strength increases considerably.

Electrostatic interactions may be reduced by increasing the ionic strength of the solution. This has the effect of screening, and thereby reducing, all electrostatic interactions, both attractive and repulsive. When attractive interactions are generated between the surface of the adsorbent and the adsorbate, and the surface concentration is sufficiently low, an increase in ionic strength will decrease adsorption. Conversely, if non-electrostatic forces govern adsorption and the electrostatic interaction is repulsive, or at high surface concentrations, adsorption will increase with increased

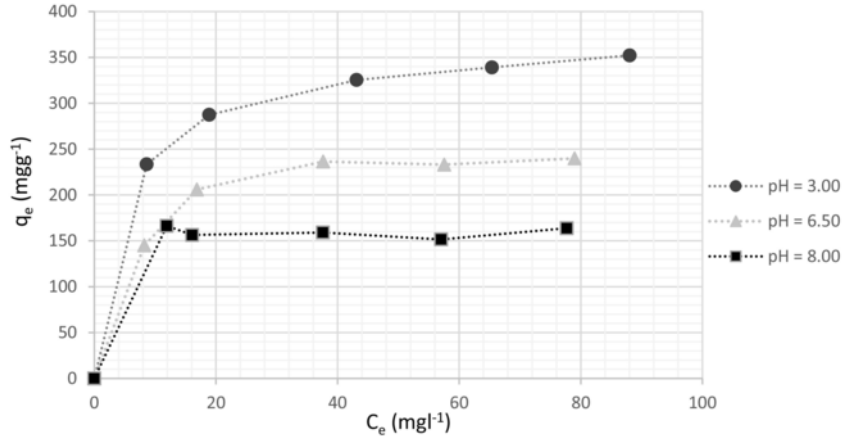

Fig. 3. 2.4–D adsorption isotherms on GAB at different pH and an ionic strength of 0.01 M.

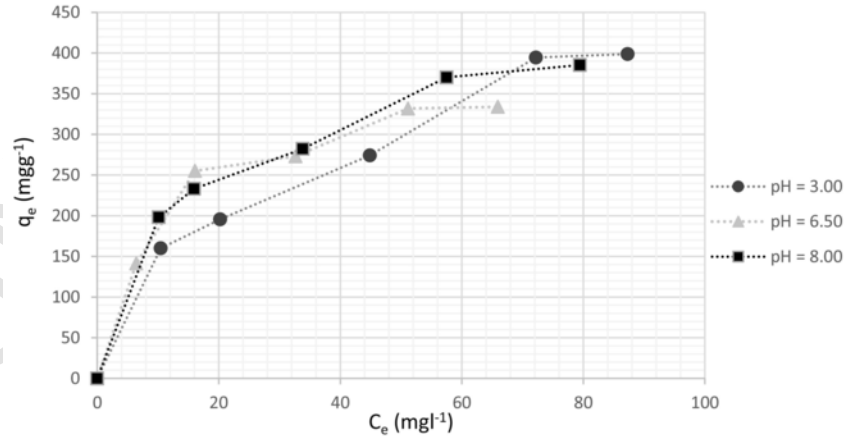

Fig. 4. 2.4–D adsorption isotherms on GAB at different pH and an ionic strength of 0.50 M.

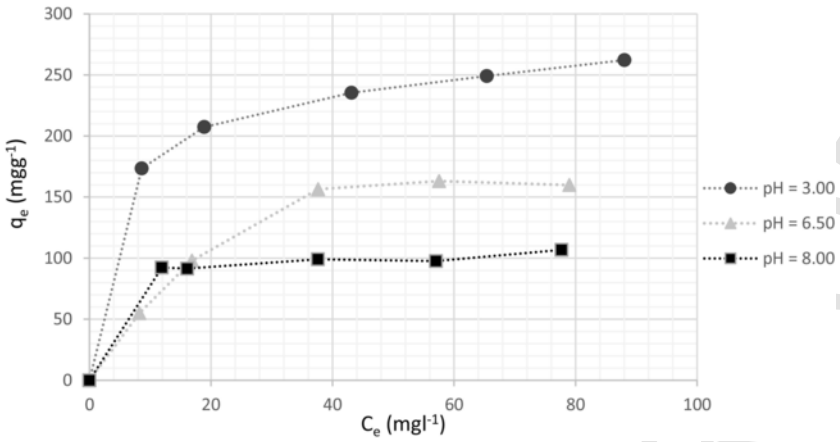

Fig. 5. 2.4–D adsorption isotherms on CBP at different pH and an ionic strength of 0.01 M.

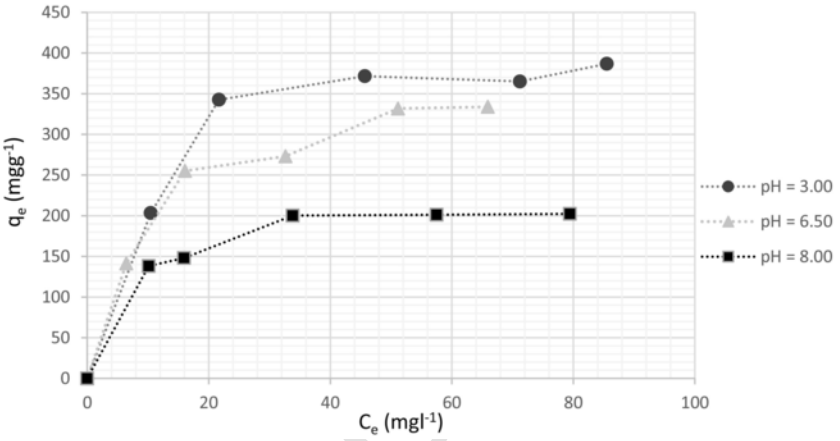

Fig. 6. 2.4–D adsorption isotherms on CBP at different pH and an ionic strength of 0.50 M.

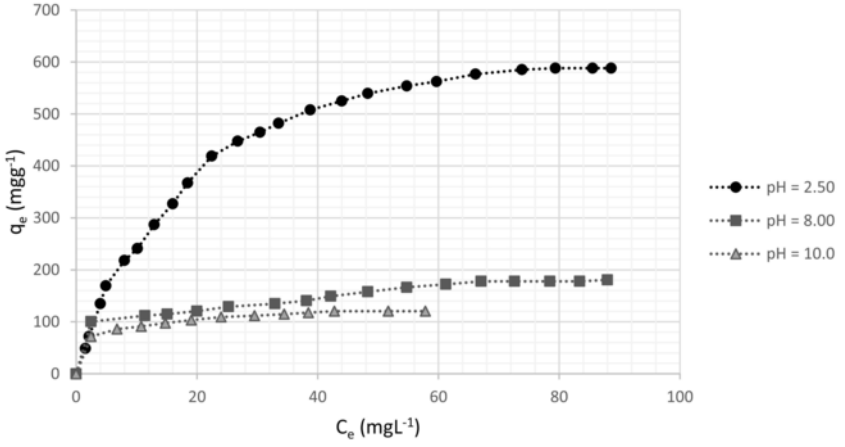

Fig. 7. MCPA adsorption isotherms on GAB at different pH and an ionic strength of 0.01 M.

ionic strength (Newcombe and Drikas, 1997; Germán-Heins and Flury, 2000).

The adsorption isotherms of 2.4 - D can be classified as L-2, according to Giles classification (Giles et al., 1960), which indicates that, as more sites in the substrate are filled with the adsorbate, it becomes increasingly difficult for the solute molecules find an active site available.

The isotherms obtained under the conditions of 0.01 M and pH = 5.00 on both materials were parametrized according to the Langmuir and Freundlich models. Table 4 summarizes the experimental values obtained according to the adjustments to these models for 2.4 – D.

The experimental data for 2.4 - D were successfully fitted by both models (Freundlich and Langmuir) for GAB adsorption, The adsorption process seems to occur in two stages: an initial step in which the pesticide is rapidly adsorbed by physical bonds and later, a slower stage, where the diffusion of the compound occurs into the less accessible active sites of the adsorbent, involving the

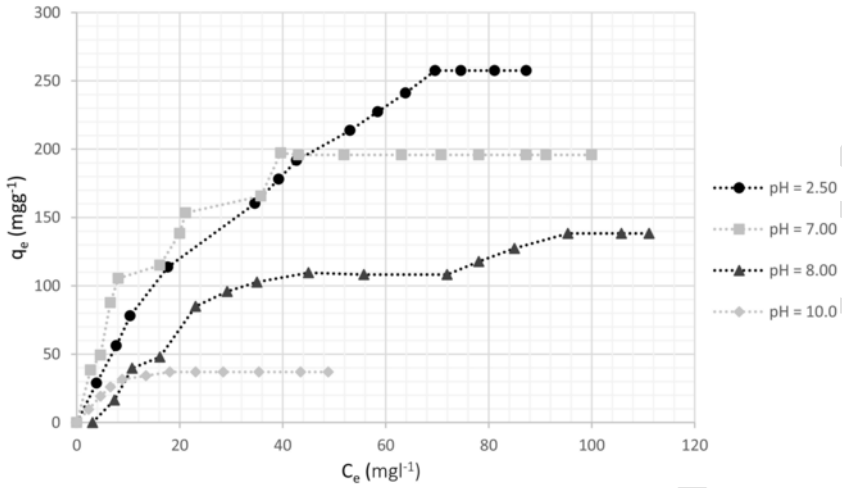

Fig. 8. MCPA adsorption isotherms on CBP at different pH and an ionic strength of 0.01 M.

Table 4
Parameters obtained from for the adsorption of 2.4 – D on GAB and CPB.

Theoreticalmodel	GAB		CPB	
	Parameter	Value	Parameter	Value
Langmuir	Q_m (mgg^{-1})	367.1519	Q_m (mgg^{-1})	273.0683
	K_L (lmg^{-1})	0.1976	K_L (lmg^{-1})	0.1858
	R^2	0.9993	R^2	0.9959
Freundlich	K_F (mgg^{-1})	170.5971	K_F (mgg^{-1})	124.5251
	n_F	6.0422	n_F	6.0182
	R^2	0.9959	R^2	0.9987

formation of chemical bonding. Onto CBP, the best model was Freundlich, which considers that the adsorbate-adsorbent system is heterogeneous, the most commonly found in liquid-phase adsorption.

MCPA adsorption capacity values onto both tested activated carbons were found very high. This could be explained considering the molecular structure of MCPA. The molecule presents an acidic group that can form strong H-bonding with the surface of the carbonaceous adsorbents. In addition, the accessibility of the molecule into the inner pores of the carbon structure led to a faster adsorption kinetic.

Figures 7and 8 show adsorption isotherms of MCPA onto GAB and Figs. 9 and 10 on CBP under the same experimental conditions used for 2.4 – D.

The adsorption isotherms of MCPA can be classified as L-2, according to Giles classification, which indicates that, as more sites in the substrate are filled with the adsorbate, it becomes increasingly difficult for the solute molecules find an active site available. The isotherms obtained under the conditions of 0.01 M and pH = 3.00 on both materials were parametrized according to the Langmuir and Freundlich models. Table 5 summarizes the experimental values obtained according to the adjustments to these models for MCPA.

Based on the non-linear correlation factors, the model that best suits this system is that of Langmuir. The low value of K_L, which represents the affinity constant, indicates that the strength with which an adsorbate molecule is retained on the surface of the solid is weak at this temperature. This also allows us to suppose that the forces acting on this system are of a physical nature. For MCPA, the adsorption capacity onto CBP activated carbon was lower than that obtained for GAB activated carbon. Onto CBP, the best model was Langmuir although Freundlich isotherm model is also goof fitted, which considers that the adsorbate-adsorbent system is heterogeneous, the most commonly found in liquid-phase adsorption. The adsorption process seems to occur in two stages: an initial step in which the pesticide is rapidly adsorbed by physical bonds and later, a slower stage, where the diffusion of the compound occurs into the less accessible active sites of the adsorbent, involving the formation of chemical bonding. In this case, when the pH solution increased, the adsorption capacity decreased.

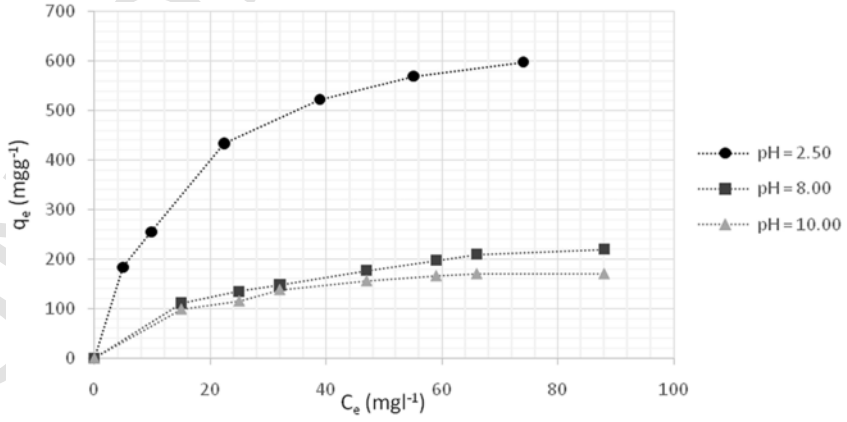

Fig. 9. MCPA adsorption isotherms on GAB at different pH and an ionic strength of 0.50 M.

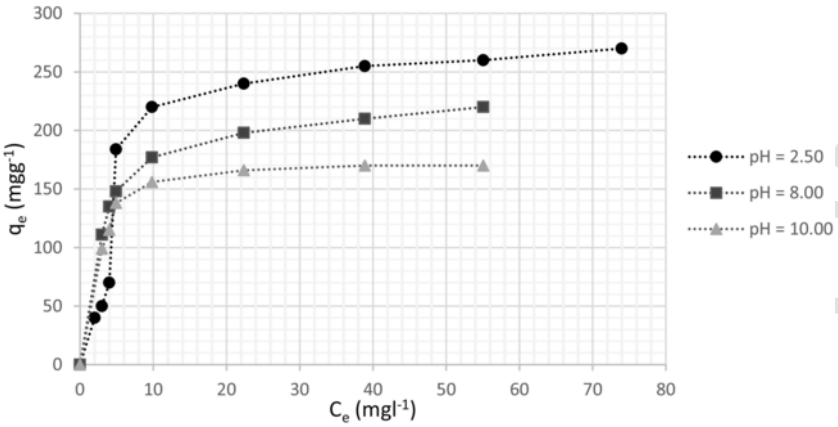

Fig. 10. MCPA adsorption isotherms on CBP at different pH and an ionic strength of 0.50 M.

Table 5
Parameters obtained from for the adsorption of MCPA on GAB and CPB.

Theoreticalmodel	GAB		CPB	
	Parameter	Value	Parameter	Value
Langmuir	Q_m (mgg^{-1})	599,8785	Q_m (mgg^{-1})	399,865
	K_L (lmg^{-1})	0,0285	K_L (lmg^{-1})	0,0285
	R^2	0,9955	R^2	0,9897
Freundlich	K_F (mgg^{-1})	10,4226	K_F (mgg^{-1})	125,6556
	n_F	0,8543	n_F	0,8525
	R^2	0,9656	R^2	0,9840

The results of the adsorption experiments carried out with the activated carbons, allowed to determine the best conditions to carry out the best process of removal of each pesticide.

3.3. Computational results

Several initial configurations are considered in order to find the most favorable pesticides adsorption geometry on the activated carbon surface. Upon full structural optimization, the most stables configurations are found (Fig. 11).Both molecules adsorb quasi planar on the surface. The adsorption is weak and then physique sorption is present. No significant changes are observed in the geometry of the molecules during the interaction with the surface.

We have computed the density of states (DOS) of the systems when the molecules adsorbs on activated carbon surface (Fig. 12). In addition, the densities of states of the clean surface (without the adsorbed molecules) and the isolated molecule (2.4-D or MCPA) are also shown. There are bands associated with the interaction between the molecule and surface orbitals. Both 2.4-D and MCPA activated carbon systems look quite similar. The difference on isolated molecules DOS is presented from −22.65 eV to −15.10 eV. On the other hand, the molecule-surface overlapping takes mainly play from −23.00 eV to the Fermi level and the molecules contribute with new states in the high part of the band in the range of −23.00 eV to 28.00 eV.

The electron distribution on 2.4-D and MCPA influences on the interaction with the carbon surface. In order to correlate, in same way, charge changes to adsorption effectiveness, we have performed the Bader charge analysis of both molecules. Tables 6 and 7 show the charge changes on individual atoms of 2.4-D and MCPA molecules, respectively, according to Bader space-partitioning scheme (the major changes are in bold). The electron on benzene ring of 2.4-D are mainly implies in the interactions with the carbon surface. The increased π-electron density strengthened the attraction between benzene ring of 2.4-D and graphene through π-π interaction. Similar interaction is present during MCPA adsorption; in addition, O—C and H—C interactions are also present.

4. Conclusions

GAB activated carbon is the material that has the highest adsorption capacity for both the MCPA and 2.4 - D. This can be explained, not only by its high specific surface (although less than CBP), but its basic properties given by us point of zero charge. The increase of external factors such as pH and ionic strength, generate a decrease in the capacity of adsorption within the studies for the MCPA, but in the case of 2.4 D, the increase in the ionic strength increases the capacity of adsorption. Theoretical, for 2.4 – D adsorption analysis, experimental data fitted with both classic models (Langmuir and Freundlich) on GAB and CPB, and MCPA shows a better fitted with Langmuir model on GAB and CPB.

Considering computational work, calculations signified that the adsorption reaction is spontaneous, exothermic and weak. The π-π interaction between benzene ring of 2.4-D (or MCPA) and grapheme layer is an important factor that resulted in the molecule adsorption. In addition, O—C and H—C interactions are also present during MCPA adsorption.

Supplementary data to this article can be found online at https://doi.org/10.1016/j.jconhyd.2018.10.003.

Acknowledgements

Financial support is highly acknowledged to Facultad de Ciencias Exactas-UNLP (Universidad Nacional de La Plata, Buenos Aires, Argentina), UTN (Universidad Tecnológica Nacional), UNS (Universidad Nacional del Sur), CONICET (Consejo Nacional de Investigaciones Científicas y Técnicas) and CIC BA (Comisión de Investigaciones Científicas de la Provincia de Buenos Aires). S. Simon-

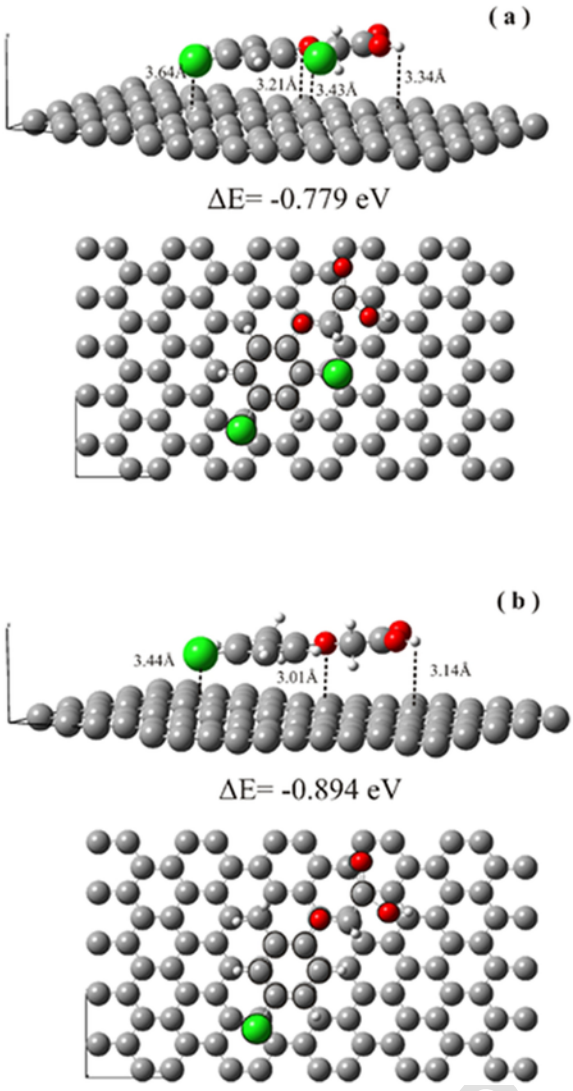

Fig. 11. Lateral and top views of 2.4 – D (a) and MCPA (b) adsorbed on the activated carbon surface.

etti, D. Ruiz and A. Juan are members of CONICET. A. Díaz Compañy is member of CIC BA. The authors declare that they have no conflict of interest.

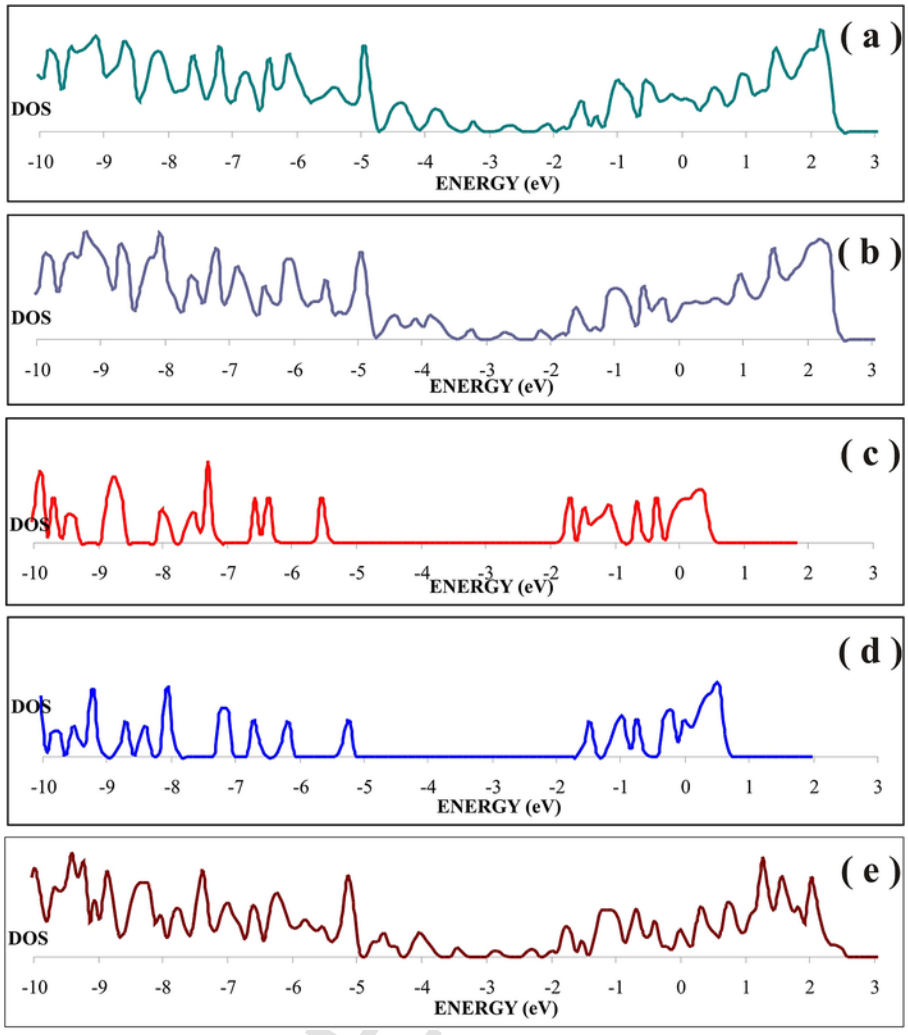

Fig. 12. Density of states (DOS) for (a) 2,4-D on AC, (b) MCPA on AC, (c) isolated 2,4-D molecule, (d) isolated MCPA molecule and (e) clean AC surface.

Table 6
Partial charge on atoms for isolated and adsorbed 2,4-D molecule on the activated carbon surface (AC) surface.

Atom	Isolated 2,4-D	2,4-D on AC	Charge exchange
1	4.1742	4.0238	−0.1504
2	3.7734	3.7970	0.0236
3	4.0131	3.9268	−0.0863
4	3.1959	3.2869	0.0910
5	3.9385	3.9638	0.0253
6	3.8874	4.0222	0.1348
7	3.2993	3.3209	0.0216
8	1.2649	1.2657	0.0008
9	7.9065	7.9253	0.0188
10	7.6286	7.6345	0.0059
11	7.8988	7.8956	−0.0032
12	0.8891	0.9053	0.0162
13	0.9165	0.8657	−0.0508
14	0.9117	0.8963	−0.0154
15	0.0002	0.0005	0.0003
16	0.9113	0.9125	0.0012
17	0.9537	0.9417	−0.0120
18	7.2250	7.2260	0.0010
19	7.2119	7.2092	−0.0027

Table 7
Partial charge on atoms for isolated and adsorbed MCPA molecule on the activated carbon surface (AC) surface.

Atom	Isolated MCPA	MCPA on AC	Charge exchange
1	4.0206	3.9941	−0.0265
2	3.8153	3.8649	0.0496
3	40,191	4.0078	−0.0113
4	32,160	3.3187	0.1027
5	4.0724	3.8526	−0.2198
6	4.0066	4.0427	0.0361
7	4.0128	4.0773	0.0645
8	3.2845	3.2526	−0.0319
9	1.2945	1.2431	−0.0514
10	7.6220	7.5882	−0.0338
11	7.8639	7.9679	0.1040
12	7.9203	7.9146	−0.0057
13	0.0002	0.0002	0.0000
14	0.9259	0.9280	0.0021
15	0.9400	0.9331	−0.0069
16	0.9508	0.8898	−0.0610
17	0.9555	0.9718	0.0163
18	0.9977	0.9906	−0.0071
19	0.9693	1.0021	0.0328
20	0.9455	0.9322	−0.0133
21	0.9278	1.0082	0.0804
22	7.2394	7.2381	−0.0013

References

Babic, B.M., Milonjic, S.M., Polovina, M.J., Kaludierovic, B.V., 1999. Point of zero charge and intrinsic equilibrium constants of activated carbon cloth. Carbon 37, 477–481.

Bader, R.F.W., 1990. Atoms in Molecules: A Quantum Theory, A Clarendon Press Publication International Series of Monographs on Chemistry. Oxford University Press, Oxford.

Barrett, E.P., Joyner, L.G., Halenda, P.P., 1951. The determination of pore volume and area distributions in porous substances. II. Comparison between nitrogen isotherm and mercury porosimeter methods. J. Am. Chem. Soc. 73, 3155–3158.

Bautista-Toledo, I., Ferro-García, M.A., Rivera-Utrilla, J., Moreno-Castilla, C., Vegas Fernández, F.J., 2005. Bisphenol A removal from water by activated carbon. Effects of carbon characteristics and solution chemistry. Environ. Sci. Technol. 39, 6246–6250.

Bloch, P., 1994. Projector augmented-wave method. Phys. Rev. B 50, 17953–17979.

Boehm, H., 1994. Some aspects of the surface chemistry of carbon blacks and other carbons. Carbon 32, 759–769.

Buckles, R.E., Wawzonek, S., 1948. Small scale synthesis of 2,4-dichlorophenoxyacetic acid. J. Chem. Educ. 25 (9), 514.

Budaver, S., 1989. The Merck Index, 11th ed. Merck & Co, Inc.

Chen Nand Yang, R.T., 1998. Ab initio molecular orbital calculation on graphite: Selection of molecular system and model chemistry. Carbon 36, 1061–1070.

Chen, N., Yang, R.T., 1998. Ab initio molecular orbital study of the unified mechanism and pathways for gas−carbon reactions. J. Chem. Phys. A 102 (31), 6348–6356.

EPA, 2007. Federal Register: 2.4-D, 2.4-DP, and 2.4-DB, Decision Not to Initiate Special Review. In: www.epa.gov/fedrgstr/EPA-PEST/2007/August/Day-08/p15109.

Fielding, M., Barcelò, D., Helweg, A., Galassi, S., Torstensson, L., van Zoonen, P., Wolter, R., Angeletti, G., 1992. Water Pollution Research Reports, No. 27. Commission of the European Communities, Brussels, 1–136.

Forest Health Protection, 2006. 2,4-D human health and ecological risk assessment final report. USDA Forest Service, Arlington, xv–xxiv.

Galarneau, A., Villemo, F., Rodriguez, J., Fajula, F., Coasne, B., 2014. Validity of the t-plot method to assess microporosity in hierarchical micro/mesoporous materials. Langmuir 30, 13266–13274.

Germán-Heins, J., Flury, M., 2000. Sorption of Brilliant Blue FCF in soils as affected by pH and ionic strength. Geoderma 97, 87–101.

Giles, C.H., MacEwan, T.H., Nakhwa, S.N., Smith, D., 1960. Studies in adsorption. Part XI. A system of classification of solution adsorption isotherms, and its use in diagnosis of adsorption mechanisms and in measurement of specific surface areas of solids. J. Chem. Soc. 3973–3993.

Grimme, S., 2006. Semiempirical GGA-type density functional constructed with a long-range dispersion correction. J. Comput. Chem. 27, 1787–1799.

http://www.vasp.at/.

IARC monographs on the evaluation of carcinogenic risks to humans: an updating of IARCMonographs, Supplement 7. Lyon, France: WHO; 1987:1–42.

Janiak, C., Hoffmann, R.R., Sjovall, P., Kasemo, B., 1993. The potassium promoter function in the oxidation of graphite: an experimental and theoretical study. Langmuir 9, 3427–3440.

Kobylecka, J., Ptaszynski, B., Rogaczewski, R., Turek, A., 2003. Phenoxyalkanoic acid complexes. Part I. Complexes of lead(II), cadmium(II) and copper(II) with 4-chloro-2-methylphenoxyacetic acid (MCPA). Thermochim. Acta 407, 25–31.

Kresse, G., Hafner, J., 1993. Ab initio molecular dynamics for liquid metals. Phys. Rev. B 47, 558–561.

Kresse, G., Hafner, J., 1993. Ab initio molecular dynamics for open-shell transition metals. Phys. Rev. B 48, 13115–13118.

Kresse, G., Hafner, J., 1994. Ab initio molecular-dynamics simulation of the liquid-metal–amorphous-semiconductor transition in germanium. J. Phys. Rev. B 49, 14251–14269.

Kresse, G., Joubert, D., 1999. From ultrasoft pseudopotentials to the projector augmented-wave method. Phys. Rev. B 59, 1758–1775.

Kruszynski, R., Bartczak, T.J., Ptaszynski, B., Turek, A., 2002. A novel lead-bis (4-chloro-2-methylphenoxy)-acetate polymeric complex. J. Coord. Chem. 55, 1079–1089.

Lamoen, D., BNJ, Persson, 1998. Adsorption of potassium and oxygen on graphite: a theoretical study. J. Chem. Phys. 108, 3332–3341.

Newcombe, G., Drikas, M., 1997. Adsorption of NOM onto activated carbon: Electrostatic and non-electrostatic effects. Carbon 35, 1239–1250.

Organic Syntheses, 1973. Coll. 5. 251, 46, (1966) 28.

Pego, M., Carvalo, J., Guedes, D., 2017. Surface modifications of activated carbon and its impact on application. Surf. Rev. Lett. 1830006, 1–10.

Perdew, J.P., Chevary, J.A., Vosko, S.H., Jackson, K.A., Pederson, M.R., Singh, D.J., Fiolhais, C., 1992. Atoms, molecules, solids, and surfaces: Applications of the generalized gradient approximation for exchange and correlation. Phys. Rev. B 46, 6671–6687.

Perdew, J.P., Chevary, J.A., Vosko, S.H., Jackson, K.A., Pederson, M.R., Singh, D.J., Fiolhais, C., 1993. Erratum: atoms, molecules, solids, and surfaces: applications of the generalized gradient approximation for exchange and correlation. Phys. Rev. B 48, 4978.

Pliego, J.R., Resende, S.M., Humeres, E., 2005. Chemisorption of SO_2 on graphite surface: a theoretical ab initio and ideal lattice gas model study. Chem. Phys. 314, 127–133.

Thomson, K.T., Gubbins, K.E., 2000. Modeling structural morphology of microporous carbons by reverse monte carlo. Langmuir 16, 5761–5773.

Tomlin, C., 1994. The Pesticide Manual, 10th Edition The Bath Press, Bath, UK, 639.

Zhu, Z.H., Lu, G.Q., 2004. Comparative study of Li, Na, and K adsorptions on graphite by using ab initio method. Langmuir 20, 10751–10755.

Both pesticides were synthesized from bibliographic data (Budaver, 1989; Organic Syntheses, 1973; Buckles and Wawzonek, 1948) and purified by recrystallization from water until verifying that their physical constants are constant and by checking into an HP5890 Gas Chromatograph coupled to an HP 5972 and a mass selective detector with an HP5-MS column, 30 m × 0.25 mm × 5 μm, using helium as a carrier gas and a flow rate of 0.6 ml·min^{-1}. Molecular structures and acid-base equilibrium of both substances are shown in Fig. 1 and the dissociation diagrams are shown in Fig. 1, where it can be observed that the pKa values of 2.4-D and MCPA were of 2.73 and 3.07, respectively. Finally, the most important physicochemical properties of both pesticides are summarized in Table 1.

The morphological characterization of activated carbons has been studied by SEM technique. Fig. S2 in the Supplementary Material show the SEM micrographs of both GAB and CBP activated carbons.

TGA curves of both activated carbons can be observed in Fig. S3 (see Supplementary Material). In the temperature range between 80 and 100 °C, the weight loss is attributed to the dehydration of the materials, characteristic of all the solids studied by this technique. The loss of water is very significant for both cases. Throughout the whole temperature range, reaching approximately to 900 °C, the mass loss was very low, indicating that both carbons are very thermally stable.